

# CFD MODEL FOR THE STEADY AND UNSTEADY STATE ANALYSIS OF A GAS MIXER FOR THE CALETONES OFF-GAS HANDLING SYSTEM

Lowy Gunnewiek  
Hatch Ltd., Canada

Claudio Muñoz & Máximo León  
Hatch Ltd., Chile

## ABSTRACT

*Gas mixer properties and performance are studied. This equipment has been included in the off-gas handling system proposed to the Caletones Smelter (Codelco), El Teniente Division. The gas mixer is part of the off-gas system upgrades proposed to improve the off-gas handling process of the existing acid plants, as well as helping regulate SO<sub>2</sub> emissions according to national regulations. The objective of the gas mixer is to create a uniform gas mixture and absorb flow transients while maintaining the gas temperature above its dew point. Commercial software packages GAMBIT and FLUENT are used to mesh a 3D model, and make a CFD model of the equipment. Two main scenarios are studied: (1) Steady and (2) Unsteady state flow. For scenario (1), two cases are studied: (A) A gas composition according to the future projected operation conditions of the smelter, and (B) A large difference in the gas composition between the off-gas coming from two Teniente Converters (CT) and two Peirce-Smith Converters (CPS). For scenario (2), case B is studied.*

*The steady state analysis showed that for cases (A) and (B) that the gas mixer allows the off-gas to have a unique and uniform composition and temperature at the at the outlet. Velocity distributions show high swirling flow inside the vessel, high pressure drop. In addition, the mixing time is less than the time residence time. In the unsteady state scenario, compositional and flow variations of the off-gas flow coming from the CPS are simulated for case B. The results show that the gas flow has fluctuations of pressure at the inlets of both CT and CPS converters, and that no significant changes of pressure were found at the outlet. In addition, changes in composition showed remarkable increase, during the transient flow conditions. These results show that the gas mixer acts as damping device for the off-gas handling system and thus would improve operation and conversion efficiency of the acid plants.*

## INTRODUCTION

The Caletones Smelter has five main reactors for the production of copper from concentrate. There are two Teniente Converters (CT1 and CT2) and three Peirce-Smith Converters (CPS1, CPS2 and CPS3). During operation, off-gas is produced by each converter which is collected and cleaned. Two acid plants are used to convert  $\text{SO}_2$  gas into sulphuric acid. Acid Plant 1 (PLG1) has a nominal capacity of  $170.000 \text{ Nm}^3/\text{hr}$  and Acid Plant 2 (PLG2) has a nominal capacity of  $300.000 \text{ Nm}^3/\text{hr}$ .

The performance of the current gas handling system design is very sensitive and dependant on operational changes. This means that small changes in control parameters (such as the damper open percentage and induced draft fan speed) have direct impact on the conversion efficiency of the acid plants, in terms of flow and pressure variations and especially, the  $\text{SO}_2$  concentration. To improve the performance of the gas handling system, a gas mixer has been proposed to be installed in Caletones. The objective of this equipment is to create a uniform gas mixture, and absorb fluctuations of pressure and composition during transients in the plant while maintaining the gas temperature over its dew point. The goal is to reduce emissions of off-gas into the atmosphere by the bypass stacks in the smelter when flow capacity of each acid plant is overloaded.

## METHODOLOGY

Figure 1 shows the gas mixer 3D model. The vessel has 3 duct inlets and 2 duct outlets. In this figure, designations for several parts of the gas mixer are shown.

The gas mixer is formed by a cylindrical vessel of 28 m height, and 17 m in diameter. An internal duct of 10 m in diameter and 14 m height is enclosed in the vessel. This duct directs the flow entering the vessel towards the upper part of the equipment, which is connected to the outlet ducts connected to the PLG 1 and PLG2. All inlets enter the vessel tangentially with the angle of separation between the CT1 and CT2 inlets is 122 degrees. The outlet ducts, one for each acid plant, are separated at 40 degrees. The upper part of the gas mixer has a conical shape connected to a small duct with a vacuum-break valve. The valve is used to prevent high negative pressures inside the vessel. In the lower part of the vessel there is a hopper used to collect any dust that settles out of the gas stream.

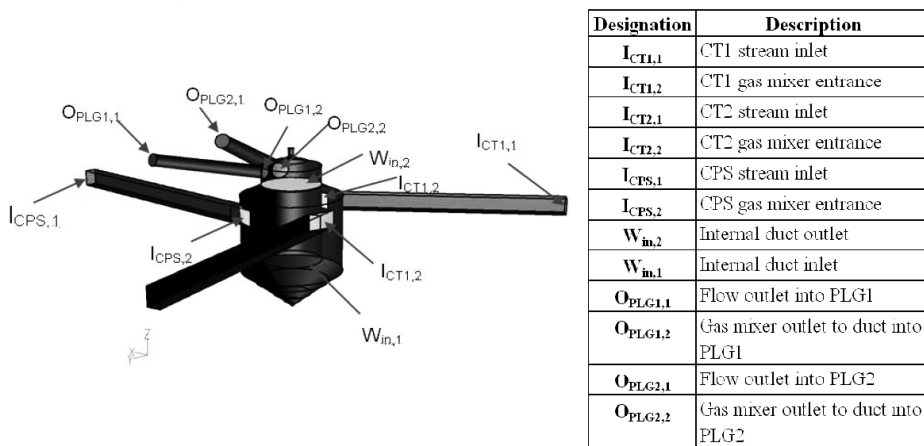


Figure 1: 3D model and designations of zones. Designations of several zones are described in the table presented on the right

Assumptions and simplifications in geometry are the following: no dampers are modeled, and the length of inlet ducts are longer than proposed in order to obtain fully developed flow conditions entering the gas mixer, and vacuum-break valve opening is not considered.

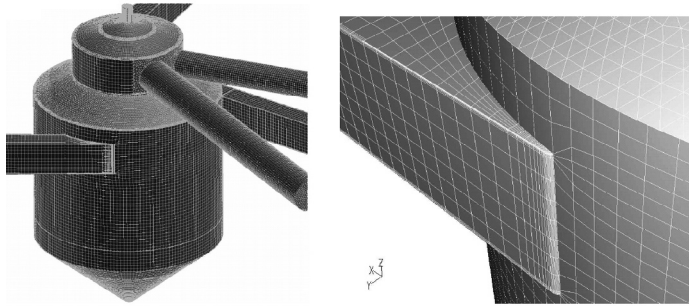


Figure 2: 3D model and designations of zones. Designations of several zones are described

Figure 2 on the right shows the 3D mesh of the model, using 500.000 elements. Inlets and the main walls of the gas mixer have been refined, using boundary layers so the wall functions for the turbulence model allows obtaining better resolution of the flow near the walls of interest. Such walls are inlet ducts, gas mixer inlets, the internal duct, and the walls of the gas mixer. Figure 2 on the left, shows details for the CT2 inlet into the gas mixer. To avoid cells with high aspect ratios and skewness, the edges in all gas mixer inlets have been rounded. This change of the geometry to accommodate gridding requirements has little impact on the results.

## Physical Models

Flow modeling is based on the realizable  $k-\varepsilon$  turbulence, considered to be suitable for this application. The energy equation is introduced in the model to consider temperature distribution in the fluid and the walls of the gas mixer. In addition, the species model is used to consider mass flux of species of each gas stream. The species included are  $\text{SO}_2$ ,  $\text{O}_2$ ,  $\text{N}_2$  and  $\text{H}_2\text{O}$  (vapor). Each stream has a composition that includes air infiltrated in the flow upstream of the gas mixer. Finally, compressible effects are neglected, since the Mach number  $M < 0.1$  [1].

## Boundary, Initial Conditions and Case Definition

### Boundary Conditions

Boundary conditions are summarized in Tables 1 and 2. Flow characteristics at inlets such as mass flow, temperature, and the respective composition of the streams are obtained from the future process scenario of the acid plants.

Turbulence intensity  $I$  levels are taken between 2.2 and 2.6% according to the levels typically used in developed turbulent flow, estimated by Equation 1 [1]:

$$I \approx 0.16(\text{Re}_{D_h})^{-1/8} \quad (1)$$

Table 1: Boundary conditions for the steady state scenario

CPS stream ( $I_{CPS,1}$ )	Condition		
	CT 1&2 streams ( $I_{CT1,1}$ & $I_{CT2,1}$ )	Exit to PLG 1 ( $O_{PLG1,1}$ )	Exit to PLG 2 ( $O_{PLG2,1}$ )
Mass flow: 64 kg/s	Mass flow: 54 kg/s	Outlet pressure: -750 Pa	Outlet pressure: -700 Pa
Temperature: 332°C	Temperature: 332°C	Temperature: 317°C	Temperature: 317°C
Turbulence intensity: 2.5%	Turbulence intensity: 2.2%	Turbulence intensity: 2.2%	Turbulence intensity: 2.6%
Hydraulic diameter: 2400 mm	Hydraulic diameter: 2400 mm	Hydraulic diameter: 2400 mm	Hydraulic diameter: 3000 mm
Composition is defined in case A and B.	SO <sub>2</sub> : 18.85% mass	SO <sub>2</sub> : 8.96 %mass	SO <sub>2</sub> : 8.96 %mass
	O <sub>2</sub> : 11.13 %mass	O <sub>2</sub> : 10.59 %mass	O <sub>2</sub> : 10.59 %mass
	H <sub>2</sub> O (steam): 8.14%mass	H <sub>2</sub> O (steam): 13.75 %mass	H <sub>2</sub> O (steam): 13.75 %mass
	N <sub>2</sub> : 61.88 %mass	N <sub>2</sub> : 66.7 %mass	N <sub>2</sub> : 66.7 %mass

Table 2: Boundary conditions for the steady state scenario. continued

Condition		
Internal duct walls	Vessel walls	Environment
Material: structural steel	Material: wool insulation	External and free stream temperature: 7°C
Thickness:8mm	Thickness:100mm	Pressure: 84820 Pa

### Initial Conditions

The initial condition for the unsteady scenario corresponds to the steady state flow conditions in the gas mixer. In time  $t=0$ , the CPS off-gas stream rapidly changes in time. This condition is set up in the model by introducing a time function for the CPS stream, in terms of mass flow rate:

$$\dot{m}_{CPS}(t) = m_f - m_0 [\tanh(k_1(t-t^*)) + 1 - e^{-k_2 t}] \quad (2)$$

Where  $t^*=0.95$  s,  $m_0=58.05$  kg/s,  $m_f=32$  kg/s,  $k^1=0.65$  s<sup>-1</sup>,  $k^2=0.5$  s<sup>-1</sup>. The mass flow rate is plotted in Figure 3. The parameters were introduced so the function has the same form of an actual transient observed in pressure measurements in the plant.

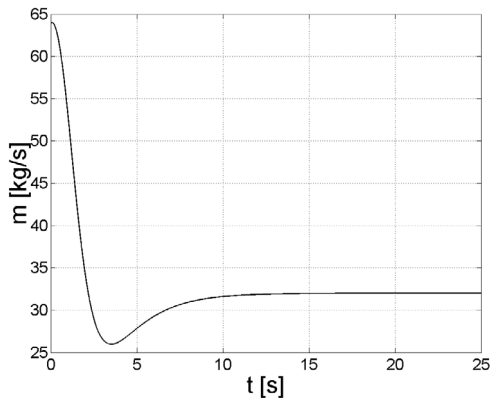


Figure 3: Mass flow rate from the CPS stream as a function of time

### Scenarios and Case Definition

The time step for the unsteady scenario will be  $10^{-3}$  s, obtained for a Courant number of 2.5. This time step provides enough time to capture the transient flow inside the gas mixer and ensures convergence of the model. Convergence is based on normalized residuals being less than  $2 \cdot 10^{-4}$ .

Table 3 summarizes the gas composition for each case. Case A is analyzed in order to obtain the gas mixer performance for the future requirements of the smelter. Case B is analyzed in order to test the properties of the gas mixer for a high variation in the inlet stream composition in order to test the mixing performance of the equipment.

Table 3: Case definition

Case	CPS off-gas composition (%mass)
A	SO <sub>2</sub> : 16.85
	O <sub>2</sub> : 11.53
	H <sub>2</sub> O (steam): 5.29
	N <sub>2</sub> : 66.33
B	SO <sub>2</sub> : 7.69
	O <sub>2</sub> : 11.05
	H <sub>2</sub> O (steam): 10.49
	N <sub>2</sub> : 70.77

## RESULTS AND DISCUSSION

### Scenario 1- Steady State Flow

#### Velocity Distribution

Figure 4 show velocity contours in several planes and flow pathlines. Two main flow zones are identified: the *Recirculation* and the *Suction* zone. The tangential inlets induce swirl in the flow, moving it counter clock-wise, hence, the name of *Recirculation zone*. Flow maintains its swirl until it enters the internal duct, incrementing its speed considerably, reaching 39 m/s in zones near the internal duct walls.

Large zones of near-zero velocities, inside the internal duct, denotes the existence of large vortex arrangements.

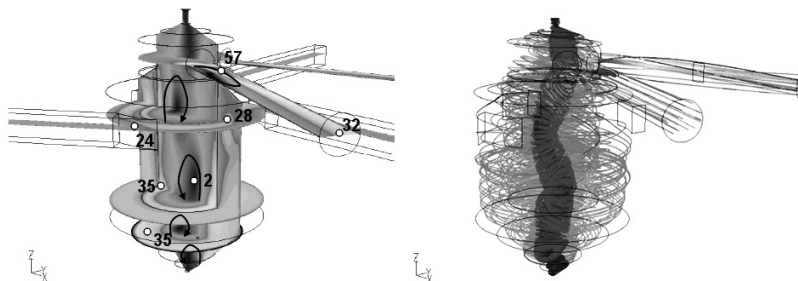


Figure 4: Left: velocity contours for case A. Representative values in m/s are indicated.  
Right: Flow pathlines. A large vortex rope-like is formed inside the internal duct

Figure 4, on the left, shows typical flow pathlines. Recirculation and horizontal vortex structures are distributed in such manner that the flow patterns follow a spiral form.

This shape has been observed in water suction produced by hydraulic turbines, in which the flow takes the form a vortex rope [3]. Therefore, the internal duct is called the *Suction zone* of the gas mixer.

Flow in the outlet ducts are characterized by a large vortex formed at the entrance, produced by the swirl of the flow inside the gas mixer. Due to this, velocities reach a maximum of 57 m/s at this location and this decrease as the flows develops inside the outlet ducts, ultimately reaching an average velocity of 25 m/s.

### Pressure Distribution

Typical pressure contours in the gas mixer are shown in Figure 5. Table 4 summarizes, for each case, the mean pressure at selected sections of the gas mixer. In addition, the net pressure drop is provided.

This high pressure drop is mainly due to formation of large vortex arrangements inside the internal duct, due to suction from the PLG's, and the swirling flow created by the flow at the gas mixer inlets. Pressure drops this high have to be overcome by the main blowers in both PLG's, with the consequent use of more energy to maintain negative pressure levels in the gas mixer.

Table 4: Mean pressure for selected sections of the gas mixer, for cases A and B

Section	Mean Pressure (Pa) Case A	Mean Pressure (Pa) Case B
$I_{CPS,2}$	-175	-149
$W_{in,1}$	-655	-645
$W_{in,2}$	-661	-651
$O_{PLG1,2}$	-1002	-1002
$\Delta P$	-827	-853

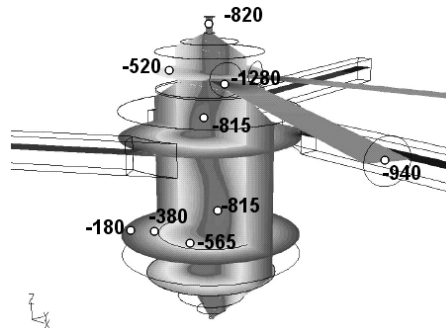


Figure 5: Pressure contours in Pa for Case A.  
The net pressure drop is approximately 830 Pa

### Wall Temperature

Figure 6 shows typical temperature contours at the inner and outer side of the gas mixer walls, respectively. The inner side of the gas mixer wall has a mean temperature of 327°C, and the outer side, 17°C.

Thus, the insulation layer is sufficient to maintain the flow temperature above the dew point of 270°C in most parts in the surface. However, attention should be paid to the

lower part of the gas mixer hoper and the small duct for the vacuum-break valve where temperatures reach approximately 290°C, and therefore the risk of corrosion increases in these areas.

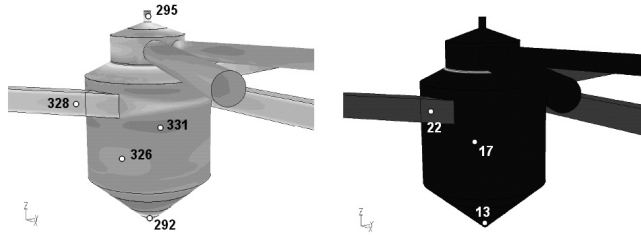


Figure 6: Contours of wall temperature in °C for case A. Left: Inner side. Right: outer side of the gas mixer walls. Representative values are indicated

**Mixing Properties**

Figure 7 show contours of SO<sub>2</sub> (in %vol) for case A (left) and B (right), respectively. A noticeable difference in SO<sub>2</sub> concentration is observed at the inlets between cases A and B and, in a big portion of the Recirculation zone.

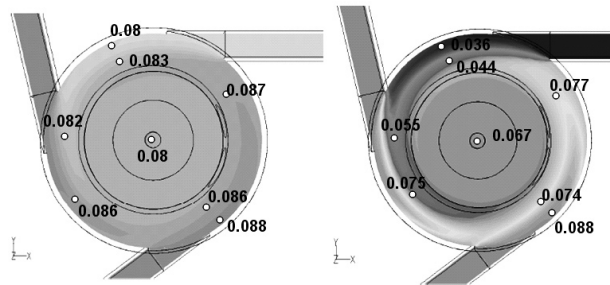


Figure 7: Contours of mole fraction of SO<sub>2</sub>: Left: case A. Right: case B. Representative values are indicated

As turbulent intensity increases, the mix becomes more uniform. In case A, uniform mix occurs shortly after the gas enters the Recirculation zone. For case B, mixing occurs near the internal duct entrance. As Figure 8 shows, further increase in turbulence intensity does not affect the gas composition.

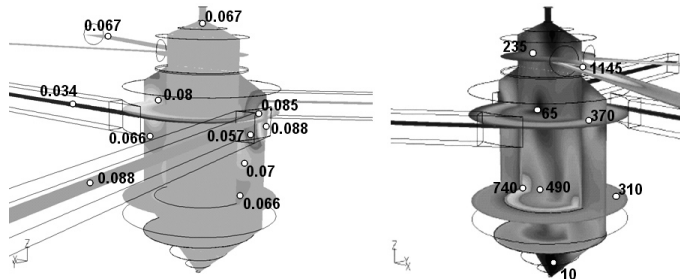


Figure 8: Left: Distribution of mole fraction of SO<sub>2</sub> for case B Right: Contours of turbulence intensity in % for case B. Representative values are indicated

**Residence Time and Mixing Time**

As previously discussed, the flow pattern inside the gas mixer and its volume describes two main characteristics. The average time for a *fluid packet* to enter and leave the gas mixer, named here as the *flying time*  $t_f$ . In most mixers systems,  $t_f$  is approximately equal to the *residence time*, estimated as  $t_f \approx V/Q$ , where  $V$  is the volume of the mixing system, and  $Q$  the flow rate entering and exiting the volume. In this model, the gas mixer volume is  $4533 \text{ m}^3$  and the average flow rate is  $325 \text{ m}^3/\text{s}$ , thus  $t_f \approx 13 \text{ sec}$ .

As seen in Figure 8 (left) for case B, composition becomes uniform near the internal duct entrance. Therefore, the mean flying time for fluid packets to reach this section of the gas mixer is different from the residence time. This situation is best explained by Figure 9, showing mole fraction of  $\text{SO}_2$ ,  $\Gamma_{\text{SO}_2}$  as a function fluid packet traveling time for two different packets in the CT1 stream. It can be inferred from these results that time to reach uniform composition is less than the time for each packet to exit the vessel at the zones denoted as  $O_{\text{PLG1,2}}$  and  $O_{\text{PLG2,2}}$  in Figure 1.

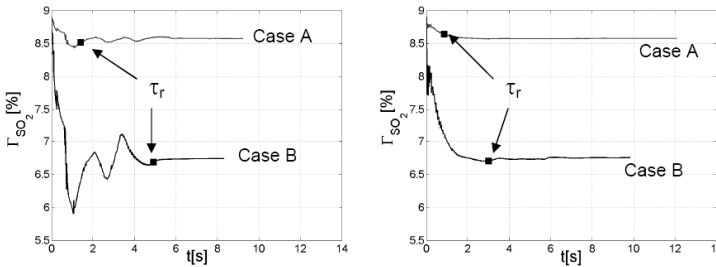


Figure 9: Mole fraction of  $\text{SO}_2$ ,  $\Gamma_{\text{SO}_2}$ , as a function of particle traveling time, for two different fluid particles, represented by figures on the left and the right

An effort to obtain an estimate of the mean mixing time,  $\tau_r$ , is performed by calculating the average time for fluid packets to reach a uniform composition. For this purpose, a total of 124 packets are released from the gas mixer inlets (zones  $I_{\text{CT1,2}}$ ,  $I_{\text{CT2,2}}$ ,  $I_{\text{CPS,2}}$  in Figure 1). For each packet, the residence time,  $\tau_r$ , is calculated as the value where root mean square (rms) fluctuations are less than 1%. Each value is stored and a *Mixing Time Distribution (MTD)* is obtained.

Figure 10 shows the MTD distribution  $E_0 = E\tau_r$ , as a function of the dimensionless time  $E_0 = t/\tau_r$ . Here,  $E$  is defined as the probability distribution, obtained from the histogram of particles reaching the  $\tau_r$  value. For case A (left), mean mixing time is 2.4 sec., and for case B (right), 4.3 sec.

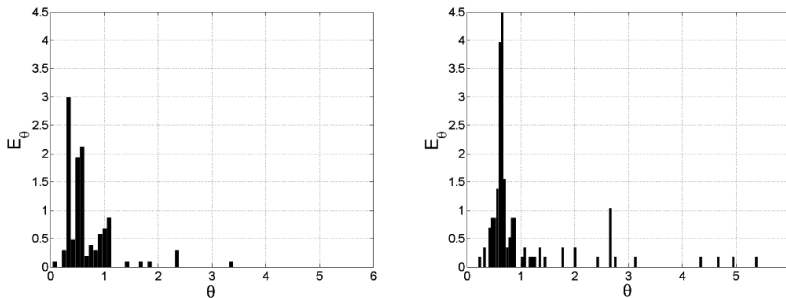


Figure 10: Normalized distribution  $E_0$  as a function of the normalized time  $\theta$ . Left: Case A,  $\tau_r = 2.4 \text{ sec}$ . Right: Case B,  $\tau_r = 4.3 \text{ sec}$

The differences in mixing times are due to the difference in composition between cases A and B. This result is supported by the composition contours shown in Figures 7 and 8. In case B, the mole fraction of  $\text{SO}_2$  becomes uniform in the vicinity of the internal duct entrance, while for case A composition becomes uniform shortly after it enters the vessel.

## Scenario 2- Unsteady Flow

### Pressure Signal

Figure 11 shows, for case B, the normalized pressure,  $\Phi = P(t)/P_0$ , at the gas mixer inlets and outlets as a function of dimensionless time  $\eta t/T$ , where  $T$  is the total simulation time. The values for the pressure at inlets,  $P(t)$ , have been normalized by the pressure at the initial condition for each inlet and outlet, that is  $P_0 = P(t=0)$ . When the mass flow is varied according to Equation 2, the pressure at the vessel inlets decreases rapidly. Pressure fluctuations are due to changes in the mean velocity patterns inside the gas mixer that, during the transient, change its direction and magnitude affecting the rest of the inlets as the flow circulates in the Recirculation zone of the gas mixer. Pressure at inlets stabilizes in a much longer time. At the gas mixer outlets, pressure decreases rapidly and at  $\eta \approx 0.13$ , it returns to a state without pressure fluctuations, with noticeable less amplitude than observed at the inlets. Thus, the gas mixer volume adds damping to the pressure signal at the inlets, stabilizing it in a relatively short time.

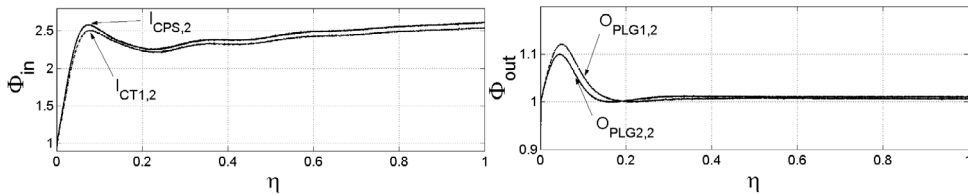


Figure 11: Comparison of the normalized pressure signal at inlets (left) and outlets of the gas mixer (Case B)

### Composition Signal

Figure 12 shows normalized mole fraction of  $\text{SO}_2$ ,  $\Gamma = \Gamma_{\text{SO}_2}(t)/\Gamma_0$ , as a function of  $\eta$ . Here,  $\Gamma_0$  is the value for the initial condition. Results show that little compositional variation occurs at the gas mixer inlets. However, at the outlets variation has an increase of 10%.

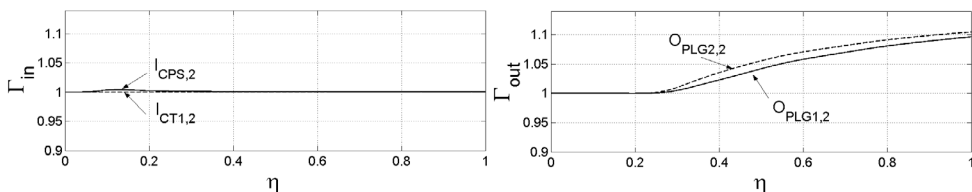


Figure 12: Comparison of normalized composition signal at inlets (left) and outlets (right) of the gas mixer

This high variation since higher pressure drop inside the Recirculation zone creates a *choking* effect in the Suction zone, preventing that, during the transient, mix becomes uniform.

In this case, and given the initial conditions, the SO<sub>2</sub> levels rise. This means that other components of the mix have increase or decrease. It is expectable that N<sub>2</sub> levels drop under this scenario, since its mole fraction is the largest. For case A, the same effect should occur, but no noticeable changes should be observed since, as shown in Figures 7 and 9, higher compositional differences implies proportional variations in the mole fraction of SO<sub>2</sub>.

## CONCLUSIONS

In summary, the study on the gas mixer has shown the equipment is suitable for the future scenario of the Caletones smelter. This equipment shows the following characteristics and performance:

- Flow patterns show high swirling flow. Two zones are defined: the *Recirculation zone*, where the mixing takes place, and the *Suction zone*, where the flow enters the internal duct, and then directed towards the upper part of the vessel. In this zone, a large vortex rope-like is created.
- Pressure drop is high due to flow patterns. This value can be decreased by changing the gas mixer overall dimensions, and varying the size of the internal duct. Mixing effectiveness will have to be evaluated will any changes in geometry.
- When a high difference in composition exists between the gas streams entering the vessel a uniform composition is only reached close to the internal duct entrance. High turbulence intensity provides the opportunity for uniform mixing. A further increase in turbulence intensity beyond that found here will not alter composition.
- The *residence time* is greater than the *mixing time*. This means that only a portion of the vessel is used to obtain uniform mix. Thus, the volume of the gas mixer is oversized in terms of its mixing properties.
- Under transient conditions, the gas mixer absorbs pressure fluctuations. This is due to the gas mixer dimensions and design, where the main flow in the *Recirculation zone* varies in pressure, and the Suction zones rapidly stabilize the flow conditions. However, for high compositional differences, it shows high variation in the SO<sub>2</sub> mole fraction.
- As a recommendation, the gas mixer should be designed, changing the geometry, in order to obtain a mixing time equal to residence time, creating a uniform mix without increasing pressure drop. Finally, the new design should balance the volume of the vessel in order to provide damping for pressure and composition fluctuations, during an off-gas flow transient.

## ACKNOWLEDGEMENTS

Support and collaboration from Codelco-El Teniente Division is greatly acknowledged.

## REFERENCES

- ANSYS<sup>TM</sup>. (2006). *Fluent User's Guide*. Ch 14, pp 1-64, ch 12, pp 1-111. [1]
- Diarra, D., Velaga, S., Lucka, K. & Köhne, H. (2006). *CFD Analysis of Mixing Systems and Residence Time Distribution in Cool Flame Vaporizers*. ECCOMAS CFD, TU Delft, The Netherlands. [2]

**Dan, G. & Sanda, M.** (2007). *Vortex Rope Investigation by 3D-PIV Method*. 2<sup>nd</sup> IAHR International Meeting of the Workgroup on Cavitation and Dynamic Problems in Hydraulic Machinery and Systems Timisoara, Romania. [3]

**Twigge-Molecey, C. & Berkley, D.** (1991). *Design for Transients*. Hatch Ltd., Smelter Process Gas Handling and Treatment. The Minerals, Metals & Materials Society. [4]

